Aust. J. Plant Physiol., 2000, **27**, 1175–1186

Application of commercially available, low-cost, miniaturised NIR spectrometers to the assessment of the sugar content of intact fruit

Kerry B. Walsh[AC], *John A. Guthrie*[B] *and Justin W. Burney*[A]

[A]Plant Sciences Group, Central Queensland University, Rockhampton, Qld 4702, Australia.
[B]Centre for Food Technology, Department of Primary Industries, Rockhampton, Qld 4702, Australia.
[C]Corresponding author; email: k.walsh@cqu.edu.au

Abstract. Recent decreases in costs, and improvements in performance, of silicon array detectors open a range of potential applications of relevance to plant physiologists, associated with spectral analysis in the visible and short-wave near infra-red (far-red) spectrum. The performance characteristics of three commercially available 'miniature' spectrometers based on silicon array detectors operating in the 650–1050-nm spectral region (MMS1 from Zeiss, S2000 from Ocean Optics, and FICS from Oriel, operated with a Larry detector) were compared with respect to the application of non-invasive prediction of sugar content of fruit using near infra-red spectroscopy (NIRS). The FICS–Larry gave the best wavelength resolution; however, the narrow slit and small pixel size of the charge-coupled device detector resulted in a very low sensitivity, and this instrumentation was not considered further. Wavelength resolution was poor with the MMS1 relative to the S2000 (e.g. full width at half maximum of the 912 nm Hg peak, 13 and 2 nm for the MMS1 and S2000, respectively), but the large pixel height of the array used in the MMS1 gave it sensitivity comparable to the S2000. The signal-to-signal standard error ratio of spectra was greater by an order of magnitude with the MMS1, relative to the S2000, at both near saturation and low light levels. Calibrations were developed using reflectance spectra of filter paper soaked in range of concentrations (0–20% w/v) of sucrose, using a modified partial least squares procedure. Calibrations developed with the MMS1 were superior to those developed using the S2000 (e.g. coefficient of correlation of 0.90 and 0.62, and standard error of cross-validation of 1.9 and 5.4%, respectively), indicating the importance of high signal to noise ratio over wavelength resolution to calibration accuracy. The design of a bench top assembly using the MMS1 for the non-invasive assessment of mesocarp sugar content of (intact) melon fruit is reported in terms of light source and angle between detector and light source, and optimisation of math treatment (derivative condition and smoothing function).

Keywords: charge-coupled device, in-line, fruit quality, miniature spectrometer, near infra-red spectroscopy, non-invasive assessment, photodiode array, resolution, sweetness.

Introduction

Throughout the past 50 years, breeding and post-harvest physiology programs associated with fruit have generally focussed on the production issues of quantity, and quality with respect to storage life and visual appearance. The consumer perceives that eating quality of fruit has decreased over this time frame. Agronomic and breeding programs can deliver fruit with improved eating quality; however, this goal has not received emphasis because of the difficulty of assessing internal attributes of every item of fruit. Various non-invasive technologies such as nuclear magnetic resonance, chlorophyll fluorescence, acoustics, and near infrared spectroscopy (NIRS) can be applied to the task of non-invasive assessment of fruit eating quality attributes. At the present time, NIRS is the most appropriate technique in terms of speed of assessment and cost.

Near infra-red spectroscopy has been applied to the non-invasive estimation of fruit eating quality, and is in commercial use in Japan (Kawano 1994). Published reports of such applications have largely involved either the use of research grade NIR instrumentation, unsuited to packing shed or field use (e.g. Guthrie and Walsh 1997; instrument value *ca* A$100 000) or the use of purpose-built spectrometers, unavailable for general application (e.g. Jaenisch *et al.* 1990; Bellon *et al.* 1993; Peiris *et al.* 1998). During the mid- to late 1990s, however, several low-cost (<A$10 000),

Abbreviations used: AOTF, acousto-optical tuneable filter; CCD, charge-coupled device; D, distance between the centre of the illuminated area and the detected area of the fruit; FWHM, full width at half maximum; InGaAs, indium gallium arsenide; IR, infra-red; MPLS, modified partial least squares; NIRS, near infra-red spectroscopy; PDA, photodiode array; R, decrease in detector response; R_c^2, regression coefficient of predicted on actual Brix for the calibration set; SEC, standard error of calibration; SECV, standard error of cross validation; SNV, standard normal variance; VR, variance ratio.

10.1071/PP99111 0310-7841/00/121175

miniature (spectrometer size <500 cm^3) array spectrometers capable of operation up to 1050 nm became commercially available. These spectrometer modules are finding use in a range of instrumentation of interest to plant physiologists (e.g. portable spectroradiometers).

Osborne *et al.* (1999) reported the use of the Zeiss MMS1 spectrometer for the prediction of sugar content of kiwifruit, and Bellon-Maurel and Vigneau (1995) reported the use of an Oriel Instaspec 2 to predict sugar content of apples, under laboratory conditions. Mowat and Poole (1997) employed an Ocean Optics S1000 and a laptop PC to discriminate between field populations of kiwifruit. However, the choice of instrumentation for the task of non-invasive assessment of fruit quality is made difficult by a lack of published specification requirements for this task. We have contributed to this field with a consideration of the wavelength resolution and signal to noise requirements of the task (Greensill and Walsh 1999). In the current paper we review the design requirements for this application, compare commercially available spectrometer modules that have been used by different researchers with respect to these criteria, and report on the design of an optical system suited to the assessment of melons.

Infra-red (IR) radiation is strongly absorbed by organic molecules, with the wavelength of absorption characteristic of the molecular bond. Overtones of the fundamental band (IR) frequencies, particularly those arising from R–H stretching modes (O–H, C–H, S–H, N–H, etc.), cause absorbance in the NIR region of the spectrum, although this absorbance is typically 10–1000 times weaker than that of the fundamental band. IR peaks are narrow and diagnostic, and thus instrumentation capable of high wavelength resolution is desirable. In contrast, peaks in the NIR spectra are broad, up to 100–150 nm wide. However, as radiation sources are readily available to deliver high intensities in the NIR region and as detectors sensitive to this region have a relatively low noise, NIRS lends itself to the quantification of organic constituents.

NIRS has been used in many fields, with most work carried out in the region of 1100–2500 nm (PbS detector). However, strong absorbance by water at around 1600 nm has restricted the use of the technique to dry materials and to reflectance optics. Hydrated objects are characterised by complicated hydrogen-bonding interactions between water, sugar, protein, etc., which complicate the spectra obtained. The application of short-wave NIR (700–1100 nm) is promising because: (1) the bands are ascribed to the third and fourth overtones of O–H and C–H stretching modes and are expected to be separated due to anharmonicity; (2) lower absorbance at these wavelengths allows for transmission optics; and (3) the corresponding instrumentation is low-cost and suited to process control, and portable enough for *in situ* field measurements. The ability to collect and interpret spectra of hydrated objects using short-wave NIR has blossomed in the past decade, with advances in detector arrays, fibre optics and personal computing power.

Unfortunately, due to the complexity of NIR spectra (band overlaps), relatively sophisticated chemometric procedures (data processing such as derivatives, and data analysis using multiple linear, partial least squares or neural network regression techniques) are required for spectral analysis. Spectral data can easily be over-fitted in the regression analysis. The resultant calibration is useful for predictions within the populations from which it was developed, but can fail when used on new populations (i.e. the calibration is not robust). Instrumentation drift over time can also result in prediction failure, and differences between instrument units can preclude calibration transfer between instruments.

The design of the spectrometer can be rationalised with respect to the application. For example, given the broad character of the absorption peaks in the NIR region, it is possible that spectral resolution may be traded off to increase detector sensitivity (i.e. a wider slit, or wider pixels). Spectral resolution may be determined by pixel dispersion (the range of wavelengths divided by the number of pixels), but is otherwise a function of slit width as well as the quality of the dispersive element (e.g. density of lines on grating). Further, the dispersive element may be chosen with transmissivity characteristic, rather than wavelength resolution, as the primary feature. The type of detector should also be considered with respect to the application requirements. Silicon detectors are sensitive into the NIR spectrum up to about 1100 nm, while indium gallium arsenide (InGaAs) detectors are useful over the 900–1700 nm spectral region. However, silicon detectors are preferred for reasons of cost and signal to noise ratio. Photodiode silicon detectors are approximately 100 times less sensitive to light than charge-coupled device silicon detectors, but the higher saturation level of the photodiode supports a 10-fold higher maximum signal to noise ratio for this detector, relative to charge-coupled device (CCD) detectors (i.e. 10 000 *cf.* 1000). Overall, CCDs are preferred for very low light applications, while photodiodes are the better choice for accurate absorbance measurements when higher light levels are available (Oriel 1997). However, signal per detector pixel can be increased by increasing the height of the pixel and slit, by focussing light from a high slit onto the array or by summing columns in a two-dimensional array.

The specification requirement for a spectrometer to support NIRS assessment of fruit in an in-line or field setting includes high signal to noise ratio, relatively high sensitivity (particularly if complete transmission spectroscopy is intended), and tolerance to vibration and dust. In-line application also requires the capacity for rapid spectral acquisition, with assessment of up to 10 pieces of fruit s^{-1}. Scanning grating instruments, with light detected by a single detector, are too slow in this respect, and are also vibration-sensitive in terms of wavelength calibration. A stationary

dispersive element and a fixed detector array can be very robust in terms of wavelength reproducibility, and very rapid in terms of spectra acquisition. Therefore, the typical spectrometer for the in-line sorting of fruit will consist of an entrance slit (with an inverse relationship between spectrometer sensitivity and wavelength resolution), a dispersive element (prism, grating or acousto-optical tuneable filter, AOTF), a fixed array detector (linear silicon or indium-gallium-arsenide photodiode array, PDA; or linear or two-dimensional CCD array), and an analogue to digital conversion device (usually 8–16 bit, i.e. a grey scale of 256–65536 levels, typically up to the dynamic range — maximum signal/detection limit — of the instrument).

A grating is the usual choice for the dispersive element, blazed at a wavelength in the NIR to maximise the efficiency of light transmission in this range, although the spectrometer used by Dull *et al.* (1989, 1992; to assess melon soluble solids content) and Peiris *et al.* (1998; to assess peach soluble solids content) utilised an AOTF as the dispersive element. The detector is usually either a silicon PDA [as in the Zeiss MMS1, as used by Osborne *et al.* (1999); and the Oriel Instaspec 2, as used by Bellon-Maurel and Vigneau (1995)], or a linear CCD array [as in the Ocean Optics S1000, as used by Mowat and Poole (1997)]. Bellon *et al.* (1993) described the application of a 2-dimensional CCD array, comprised of 500 × 582 pixels (pixels 17 × 11 μm). A grating was used to disperse the light such that rows represent spectra, and columns were averaged to increase the signal to noise ratio. The Oriel FICS unit is capable of accepting various detectors, but is optimally used with a 2500 μm high (PDA) detector. As costs decrease, InGaAs arrays will offer potential, operating over the wavelength range 900–1700 nm.

The spectral response, and the stability of this response, of a spectrometer will be affected by the spectral output of the light source, transmission and reflection characteristics of the optical path within the spectrometer (e.g. entrance slit width, grating groove density), the stability of the mounting of the optical components (with respect to vibration and thermal expansion coefficients), the spectral response of the detector, and the stability of the electronics. The effect of trade-offs between wavelength resolution and decreased light levels at the detector (e.g. narrower entrance slit), and between signal to noise ratio and detector sensitivity (i.e. photodiode *cf.* CCD) encountered in the choice of NIR instrumentation, deserve attention with respect to the task of assessing the sugar content of intact fruit.

In this paper we evaluate three commercially available, low-cost NIR spectrometers that differ in terms of the aforementioned parameters, with respect to the non-invasive measurement of Brix (sugar content) of melon fruit. We also report on the optimisation of an optical configuration suited to the assessment of melons, and the optimisation of chemometric processing technique. A field portable unit has subsequently been based on this design, and melon spectra collected across growing district and time to explore calibration robustness issues.

Materials and methods

Spectrometer description

Three commercially available miniature spectrometers, with gratings chosen for operation in the NIR, were acquired — the Zeiss MMS1 (Monolithic Miniature Spectrometer, Zeiss, Jena, Germany), the Ocean Optics S2000 (Dunedin, FL, USA, distributed through LasTek, Adelaide, Australia) and the Oriel Fixed Image Compact Spectrometer (FICS; Oriel, Stratford, CT, USA, model 77443), using a Larry linear CCD array (distributed through LasTek).

The Zeiss MMS1, released in 1994, consists of a block of glass (UBK 7) with the imaging grating directly replicated onto one surface. The body thus acts as the dispersive element, and also images the entrance slit onto the diode array by varying groove density and using curved grooves to correct coma and flatten the focal curve to optimise use of the flat detector structure (6 mm long). The refractive index of the material (UBK 7) used in the construction of the body is higher than that of flint glass, giving greater angles of refraction and thus enabling the unit to be reduced in size. With the monolithic construction, the grating is immovable and thus vibration-tolerant and protected against dust, and the spectrometer is relatively tolerant of temperature changes (wavelength drift of 0.012 nm/K specified).

A fibre optic cross section converter is employed, with a linear arrangement of 30 quartz fibres (each 70 μm wide) acting as the slit for the instrument. Thus, slit width is not alterable. A Hamamatsu diode array (S3904–256Q, 256 elements, each 25 × 2500 μm, 6 mm total length) is used as the detector. With detection of wavelengths between 300 and 1150 nm, the MMS1 has a pixel dispersion of 3.3 nm pixel^{-1}. Order sorting filters are applied during manufacture to different regions of the array to eliminate detection of second order spectra over this wide wavelength range. A 12-bit analogue to digital conversion device was used, under the control of Zeiss software. The Zeiss software supplied with the MMS1 employs a smoothing function for its graphical display, but not on saved data, as used in the calculations of mean and standard error of signal in this study.

The Ocean Optics S2000, released in 1997, has increased sensitivity relative to the original 1992 release (S1000). A 2048 element linear CCD array (each 12.5 × 200 μm, 4 mm total length) is employed, with only the mid-section used to minimise problems with field distortion. To optimise use in the NIR region, an order-sorting filter (550 nm) was factory-installed. With the grating (#14, blaze 1000 nm, 600 lines mm^{-1}) and the slit width (50 μm) chosen (factory-installed), a 3 nm resolution is specified. With a nominal wavelength range of 632–1278 nm, and a number of blackened pixels, the S2000 has a pixel dispersion of 0.36 nm pixel^{-1}. A 12-bit analogue to digital conversion device was used, with data acquisition controlled by Spectra Array (LasTek).

With the Oriel, the slit is mounted on a slide, and so can be varied. A 25-μm slit was used in this study. A 2048 element linear 'Larry' CCD array (12.5 × 200 μm) was employed as the detector. With the grating (blaze 1000 nm, 600 l mm^{-1}) chosen, a wavelength range between 300 and 1150 nm was detected, giving a pixel dispersion of 0.41 nm pixel^{-1}. A 12-bit analogue to digital conversion device was used, with data acquisition controlled by Spectra Array (LasTek).

Spectrometer comparisons

The performance of the spectrometers was compared in terms of wavelength resolution and stability, relative spectral sensitivity, relative detector sensitivity, signal to noise ratio, stability over time and variation in temperature and calibration performance. To achieve these comparisons, wavelength calibration was undertaken using a mercury argon lamp (HG1, Ocean Optics), and spectra were acquired of a refer-

ence material (WS-1, halon reference, Ocean Optics) and of samples (i.e. Whatman #1104 filter paper saturated with a range of concentrations of sucrose.

Spectra of filter paper soaked with sucrose solutions were collected using a reflectance probe with six illumination fibres and one read fibre (all fibres 400 μm in diameter, R400-7, Ocean Optics). The read fibre was directed to a spectrometer, while the illumination fibres were connected to a 6-W tungsten halogen light source (LS-1, Ocean Optics). SMA connectors (NA 0.22) were used to connect these items. Spectrometer temperature was varied by placing the spectrometer within the oven of a Gas Partitioner (Model 1200; Fisher, North Ryde, Sydney, Australia) or within an ice box, and monitored by a thermocouple placed in contact with the spectrometer body. Temperature was ramped from ambient (22) to 0°C, and then increased to 45°C, at approximately 0.2°C min^{-1}.

NIRS calibration technique

Two populations [n = 40 (two spectra $fruit^{-1}$); n = 210 (one spectra $fruit^{-1}$); combined Brix range 5.4–11.2] of rockmelons (*Cucumis melo* L. cv. Dubloon) were sourced from the Bowen-Burdekin (North Queensland) region in November 1998 for use in the comparison of instrumentation. A further 10 populations (total n = 1991, two spectra $fruit^{-1}$, Brix range 4.4–12.2) of rockmelons (four cultivars, Hammersley, Eastern Star, Malibu and Dubloon, from various growing regions) were obtained during 1998 and 1999 and spectra collected using the purpose-built instrument described below. This larger data set was used in the consideration of the optimal data treatment for calibration, with the optimal data treatment then used for the calibrations involving the comparison of instrumentation reported in this paper.

Spectra acquisition and wet chemistry occurred within 3 d of harvest at the 'slip' stage (fruit breaking away from peduncle). Spectral data was acquired of an area of the fruit equidistant between point of attachment of peduncle and corolla, but not of an area that had been in contact with the ground during fruit growth. Where two spectra were acquired $fruit^{-1}$, spectra were acquired from opposite sides of the fruit. Juice was extracted of 40 mm diameter plugs of fruit mesocarp tissue underlying the assessed areas, with soluble solids concentration assessed using an Erma (Tokyo, Japan) digital refractometer. While a range of *ca* 6 Brix units was recorded between different fruits (population ranges reported above), a range of *ca* 1.5 Brix units was also recorded within the central region of a given fruit (i.e. around the 'equator' of the fruit). Brix of prepared sucrose solutions was also measured using the Erma refractometer.

Zeiss and Spectra Array files were converted to JCAMP format, and imported into the chemometric package ISI (version 3.0; Infrasoft International, Silver Springs, MD, USA). Spectral outliers were defined using the ISI critical 'GH' statistic (a measure of distance of spectral sample to population mean, based on an estimate of the Mahalanobois distance, D, calculated on principle component scores, defined as $GH = D^2/f$, where f is the number of factors in the PLS regression) set to a value of three. Analysis involved a modified partial least squares (MPLS) procedure using raw, first or second derivative absorbance data and six cross-validation groups. Standard normal variance (SNV) and detrend were used for scatter correction. The effect of the number of data points used in the derivative calculation ('gap') and the number of data points used in a smoothing routine offered in the ISI software was considered. As suggested in the ISI manual, calibrations were compared primarily on the standard error of cross validation (SECV) statistic, where SECV should not be greater than 20% greater than SEC, and attention given to the 1–VR (variance ratio, i.e. regression coefficient of predicted on actual Brix for the validation set) statistic. The standard error of calibration (SEC) and regression coefficient of predicted on actual Brix for the calibration set (R_c^2) are reported. Note that the terms SECV and 1–VR, and SEC and R_c^2, respectively, are directly related for a given population (e.g. $R_c^2 = 1 - (SEC/s.d.)^2$, where s.d. is the standard deviation of the actual Brix for the population).

Optimisation of optical configuration for the non-invasive assessment of melon fruit sugar content

Halotone lamps (12 V, 50 W, 50° light spread, aluminium reflector; Philips, Eindhoven, Holland) were used as light sources and the Zeiss MMS1 unit used as the detector. Reflectance (in which specularly reflected light is received by the detector) and partial transmission optical arrangements were trialed, as the optical density of the fruit prevented full transmission optics. The core configuration consisted of the detector fibre optic positioned to view the 'top' of the fruit (a position on the fruit equidistant from peduncle and blossom ends which was not an area of the fruit which had rested on the ground during fruit growth). Lamp(s) were positioned to illuminate the fruit at some (varied) distance from the area seen by the detector (i.e. angle between area of detection, centre of fruit and area of illumination varied).

The intensity of light received by the detector and the calibration performance (for prediction of mesocarp Brix) was considered with reference to the following variables: (i) the angle of incidence of light onto the fruit surface; (ii) the angle between detected area and illuminated area with reference to the centre of the fruit (i.e. distance between detected area of fruit and illuminated area); (iii) the number of lamps employed; (iv) the distance from detector fibre optic to fruit; (v) the presence of a shroud between detector fibre optic and fruit surface; and (vi) the duration of illumination (with respect to temperature of fruit).

Results and discussion

Wavelength accuracy and resolution

The instruments were calibrated using a mercury argon lamp, and spectra of the mercury argon lamp acquired at near saturation count at the 842.5 nm emission line (Fig. 1). The spectrum acquired with the MMS1 unit demonstrated a poor wavelength resolution relative to either the S2000 (Fig. 1) or the Oriel unit (data not shown). Second order spectral peaks were recorded with the S2000, but not the other instruments (e.g. at 1080 and 1155 nm, data not shown). The peak at 912.3 nm was chosen for further characterisation as it was isolated from other peaks in the MMS1 spectrum. Spectra

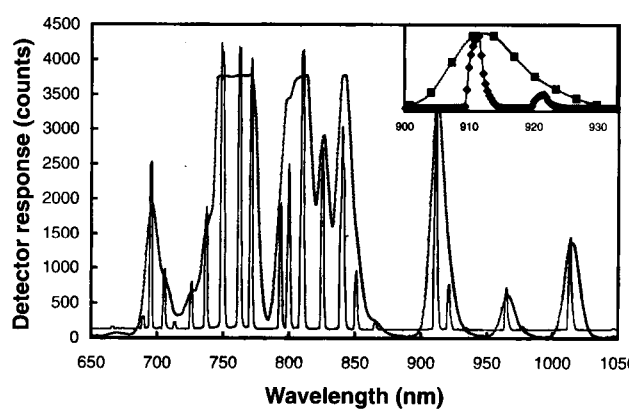

Fig. 1. Spectra of a mercury argon lamp acquired with the Zeiss MMS1 (dotted line) and the Ocean Optics S2000 (solid line) spectrometers. Inset illustrates the resolution of the 912-nm peak by the two devices (with detector response normalised to output at this wavelength).

were acquired with the count of this peak at near saturation and normalised between instruments. The line width (full width at half maximum, FWHM) of the Oriel and S2000 was 1.2 and 2.1 nm, respectively, an order of magnitude superior to the MMS1 result of 13.1 nm. These results are consistent with the slit widths, pixel dispersion and geometries of the three units.

Array spectrometers have a reputation for wavelength precision, relative to instruments in which the monochromator is a moving grating (and therefore sensitive to mechanical disturbance). The wavelength calibrations of the MMS1 and S2000 were checked periodically over a period of 6 months. During this period, the instruments were used in air-conditioned laboratories, but were subject to mild shocks and temperature fluctuations during transport between laboratories. No recalibration was necessary over this period for either instrument (i.e. measured position of 912.3 spectral line of HgAr lamp did not vary by more than 0.3 nm). However, the FWHM of array spectrometers can be sensitive to temperature, as differential expansion of materials within the spectrometer changes the geometry of the light path. The monolithic construction of the MMS1 should be advantageous in this respect. Wavelength accuracy and FWHM was stable for both the MMS1 and the S2000 over the temperature range expected in a packing shed environment. The FWHM of the MMS1 was estimated at between 13.04 and 13.13 nm, with no consistent change as the temperature of the spectrometer was varied between 4 and 45°C (data not shown). The FWHM of the S2000 varied between 2.06 and 2.12 nm as temperature was varied over this range, tending to increase with temperature (data not shown).

Relative spectral sensitivity

The three spectrometers employed silicon-based detectors, and so are expected to show decreasing sensitivity through the region 700–1100 nm, with no response beyond 1100 nm. However, the spectral sensitivity of the instrument can be altered by doping of the silicon in the detector, by use of coatings over the surface of the detector elements, and with respect to the spectral efficiency of the grating (primarily determined by the blaze wavelength). Spectra were acquired using the three instruments of the reference material in reflectance mode, using the interactance probe and a tungsten halogen light source. Spectra with a maximum count level near saturation were acquired for each spectrometer, and spectra compared after normalisation to the count at 730 nm (Fig. 2). The MMS1 was more sensitive than the other instruments over the wavelength range 750–1050 nm, and particularly over the region 800–900 nm. The Oriel–Larry unit was more sensitive at wavelengths between 650 and 700 than at 720 (data not shown). The spectrum acquired using the MMS1 was also smoother than equivalent spectra acquired with the FICS or S2000. An increase in count after 1060 nm was recorded with the S2000, a result interpreted as a second order spectra (the S2000 unit employed a 550 nm primary cut-off filter).

Spectra were recorded of the HgAr lamp using the MMS1 spectrometer, while altering the temperature of the spectrometer between 0 and 45°C (data not shown). The measured count of a 'dark' region of the HgAr lamp spectrum (870 nm) increased with temperature by a count of 0.33 $°C^{-1}$ (on a count of 29 at 0°C, linear regression, R^2 = 0.782). This increase will reduce dynamic range with temperature increase. The measured count of the 912 emission line was more responsive to temperature, increasing by a count of 10.96 $°C^{-1}$ (on a count of 2 757 at 0 °C, linear regression, R^2 = 0.913). These results are consistent with Zeiss MMS Spectral Sensor product information (79-802e), which reports a sensitivity increase of *ca* 0, 0.18, 0.47 and 0.69% $°C^{-1}$ at 500, 735, 912 and 1000 nm, respectively. Thus an increase of *ca* 12 counts $°C^{-1}$ on a count of 2757 is expected.

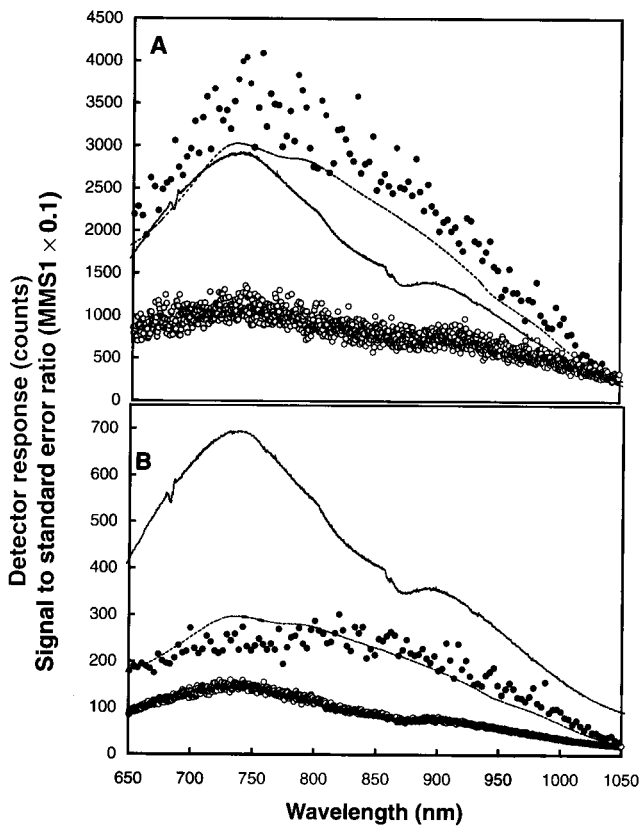

Fig. 2. Relative spectral sensitivity (lines) and signal to standard error ratio (circles) of spectra collected using the MMS1 (dashed line, solid circle) and S2000 (solid line, open circle) spectrometers. Spectra were acquired using the same integration time (100 ms), light source, fibre optic guides and sample (reference material) for the two devices. Mean signal and mean signal divided by standard error of measurement at each wavelength (n = 50) are displayed. Note the scale change for the Zeiss MMS1 signal to noise ratio. (*A*) Light intensity was adjusted such that the output of each detector was near saturation, and normalised to output at 720 nm. (*B*) Spectra were acquired on both instruments at the same, relatively low, light intensity.

Thus, detector spectral sensitivity and dark current are changing with instrument temperature. These changes may be accommodated in a field application by minimising detector temperature change, and by collecting reference and dark spectra at the same instrument temperature as experienced while collecting sample spectra.

Relative detector sensitivity

Reflectance spectra of a reference material under halogen lamp illumination were acquired using the three spectrometers at a range of probe heights (i.e. different illumination levels) but the same acquisition time spectrum^{-1} (100 ms). Regression relationships were established between the readings of the three instruments. Detector response was recorded at 735 nm, as the wavelength at which highest counts were recorded in the MMS1 and S2000 units, and also a wavelength likely to be used in calibrations developed for the sugar content of fruit (e.g. Guthrie and Walsh 1997). The S2000 gave count readings 2.65-fold higher than that of the MMS1 (R^2 = 0.998) (e.g. Fig. 2*B*), with a saturation count reached at only 25% of the range of the MMS1. In contrast, the slope of the Oriel–MMS1 regression was only 0.019 (R^2 = 0.996) (data not shown).

The sensitivity of a CCD array to light, in terms of electrons count^{-1}, is reported to be *ca* 150-fold greater than that of a PDA (Oriel 1997). The low sensitivity of the Oriel FICS assembly was primarily due to the design of the instrument optics to focus light onto a 2500 μm height (PDA) array, not onto a (CCD) detector array only 17 μm tall, as used in this study. The relatively high sensitivity of the MMS1, as a photodiode array, relative to the S2000, as a CCD array, is explained by the degree of pixel dispersion in the two units (0.36 and 3.3 nm pixel^{-1} in the S2000 and MMS1, respectively), and also by the size of the pixels in the two arrays. The MMS1 pixel (25 × 2500 μm) has an area 400-fold greater than that of the S2000 CCD (12.5 × 12.5 μm). Also, the effective slit width of the MMS1, at 70 μm (diameter of fibre optic), was greater than that employed in the S2000 (50 μm). Thus, each pixel of the MMS1 array received *ca* 150-fold greater illumination (number of photons) than in the S2000 array, for a given level of detected surface radiance.

'Signal to noise' ratio

Fifty reflectance spectra of the reference material were recorded at near saturation levels, and at a low light intensity (peak counts of >300), for each instrument. The mean was divided by the standard error of the count at each wavelength as an estimate of the signal to noise ratio. With spectra recorded at near saturation levels (3000 counts, with saturation recorded at 4096 counts on a 12-bit AtoD device) for each instrument, the maximum signal to noise ratio, recorded at peak signal count at 735 nm, was approximately 40 000, 1000 and 4000 in the MMS1, S2000 (Fig. 2*A*) and Oriel units (data not shown), respectively. At a low light level of 10% of saturation (i.e. 3000 counts) for each instrument; the maximum signal to noise ratio was approximately 3000, 250 and 400 for the MMS1, S2000 (Fig. 2*B*) and Oriel instruments (data not shown), respectively.

The total pixel noise in the signal from either the photodiode or CCD array can be approximated as the square root of the sum of squares of the followings three components: (a) read out noise, which is due to amplifier and electronics; (b) shot noise from the signal itself, equivalent to the square root of the signal; and (c) the shot noise of the dark current, which is dependent on exposure time and very dependent on temperature. The spectral shape of the noise (mean/standard error) values followed that of the signal, reflecting the importance of the signal shot noise to the total noise. The signal to noise ratio should be better for a CCD than a PDA for the operating range of the CCD, reflecting a lower read out noise, but the maximum signal to noise ratio of the PDA (achieved at higher signal levels) is expected to be an order of magnitude greater than that of the CCD (*ca* 10 000 *cf.* 1000, respectively; Oriel 1997). The result obtained with respect to maximum signal to noise of the PDA and CCD detectors was as expected. However, the signal to noise ratio was also higher for the PDA-based spectrometer than with the CCD based instruments for light levels within the range of operation of the CCD. The low noise of the MMS1 at the lower light level is therefore attributed to a low read out noise, relative to that expected for a PDA.

Bellon *et al.* (1993) estimated the signal to noise ratio of their CCD based system by dividing the spectrum of a reference material by the standard error of 10 reflectance ratios (spectrum of reference material divided by a reference spectrum of the same material) at each assessed wavelength (rather than by the standard error of the repeated raw spectra). Assuming spectra were acquired at near saturation levels, and given the use of an eight bit A/D card (i.e. saturation at a count of 256), the report of a maximum signal to noise ratio of 90 000 is equivalent to a ratio of 360 (i.e. 90000/256) in terms of the current study. Thus, the signal to noise ratio achieved by Bellon *et al.* (1993) was similar to that obtained with linear CCD arrays in the current study. This is surprising, in that as Bellon *et al.* (1993) averaged data over 512 rows, noise should have been decreased by a factor of the square root of 512 (22.6) over that of a single pixel. The difference is attributed to noisier electronics in Bellon's equipment.

Stability of spectrometer and lamp output

Using a light source that had been activated some 3 h earlier, the output of the MMS1 and S2000 was recorded with respect to time from instrument activation (Figs 3*A*, 4*A*). For the MMS1, counts generally decreased (e.g. at 750 nm, by 25 counts on 3500) (Figs 3*A*, 4*A*). The MMS1 was considered stable within 60 min of activation. In contrast, the

S2000 was relatively unstable, fluctuating by up to 3% of initial response, and not stable even after 90 min from activation. The stability of instrument response is a critical parameter in consideration of the frequency of referencing required, or the preference for a dual beam over a single beam operation.

Using a MMS1 spectrometer that had been activated some 3 h earlier, the spectral output of a tungsten halogen lamp was recorded with respect to time from activation (Figs 3*B*, 4*B*). Spectral output decreased by *ca* 5%, across most wavelengths, but increased, by *ca* 2%, at 833 nm. Most changes were complete within 30 min of lamp activation. These spectral changes are attributed to the chemistry of the tungsten halogen lamp during a warm up period following ignition. Parallel data were collected with the S2000, with trends similar to that reported above (Fig. 4*B*). The stability of the lamp output is also a critical factor in consideration of the frequency of referencing required in an application.

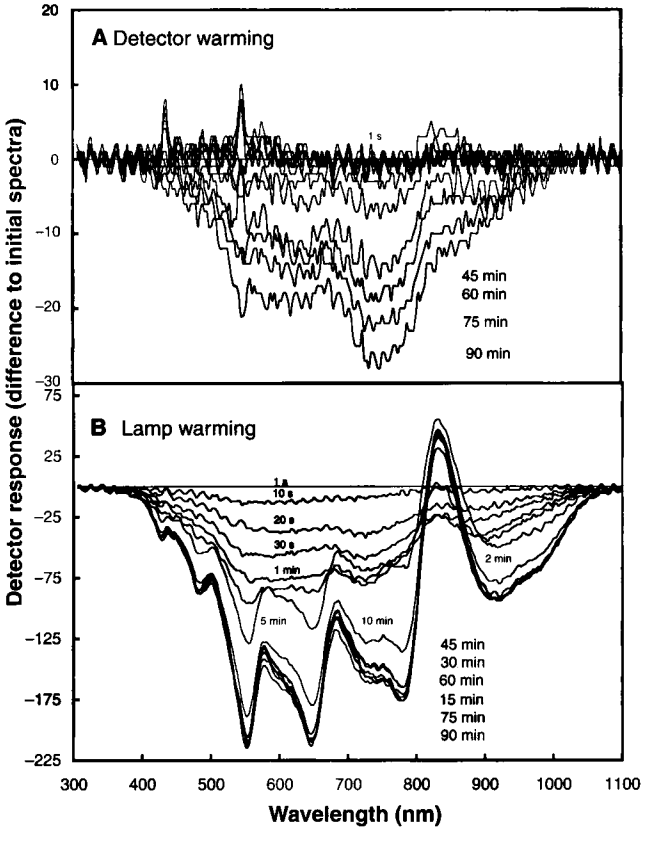

Fig. 3. The stability of (*A*) detector response and (*B*) light source, as indicated by change in spectrometer response (interactance optics, reference sample) for the wavelength range 300–1100 nm with time from instrument (detector) and lamp activation, respectively. Data are expressed as the difference in the A/D card output to that of the first spectra acquired (at 1 s after detector and lamp activation, respectively). Spectra were obtained using a halogen light source and Teflon as a reference sample.

Choice of spectrometer for the application of non-invasive sorting of fruit by NIRS

The application of fruit sorting by near infra-red spectroscopy requires an instrument that is relatively sensitive to light, in order to capture spectra of fruit in transmission or interactance modes without use of an unduly high incident radiation load (with the attendant sample heating problems). The instrument must be sensitive over the spectral region 700–1050 nm (or higher), and the detector response must be relatively stable. As noted earlier, wavelength resolution below 10 nm is probably not necessary (e.g. Greensill and Walsh 2000).

The Oriel–Larry unit gave the best wavelength resolution of the three instruments. However, its sensitivity was poor (due to the detector used), and on this basis the instrument was eliminated from consideration. The S2000 gave better wavelength resolution and detector sensitivity than the MMS1. However, the relative response of the MMS1 in the near infra-red (750–1000 nm) region was higher than in the visible region than the S2000 (Fig. 2). Further, the signal to noise ratio of the MMS1 was an order of magnitude higher than the S2000, both at high light levels (i.e. near detector

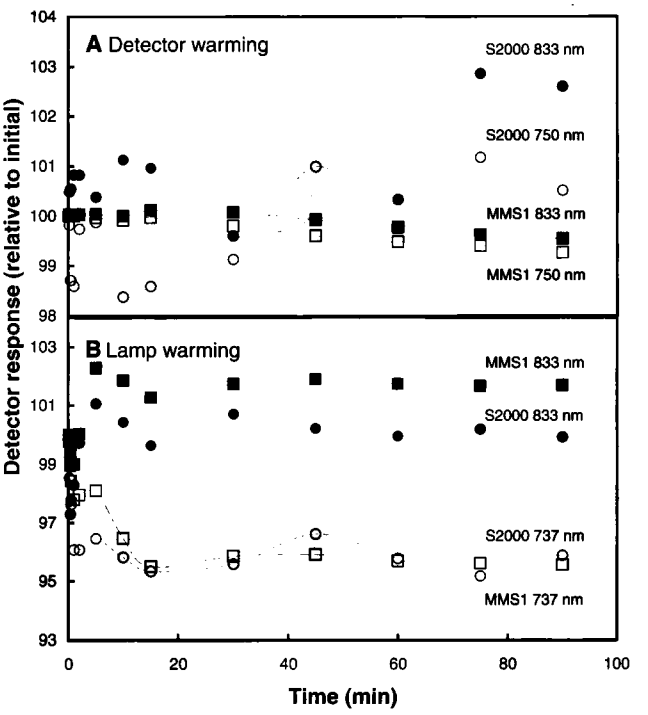

Fig. 4. The stability of (*A*) detector (MMS1, squares; S2000, circles) response and (*B*) light source, as indicated by change in spectrometer response (interactance optics, reference sample) at 750 (open symbols) and 833 nm (closed symbols) with time from instrument and lamp activation, respectively. Data are expressed as a percentage of the first record (*ca* 1 s after detector and lamp activation, respectively), and are of the same experiment as presented in Fig. 3.

saturation) and at a low light levels (within the detection range of the CCD) (Fig. 2).

To compare the spectrometers for their application to the task of assessment of fruit by NIRS, we captured spectra of filter paper saturated with sugar solutions of varying concentration in one experiment. The MMS1 supported better calibrations than the S2000 (Table 1). We conclude that the attribute of wavelength resolution was not important to the calibration process, relative to the attribute of signal to noise ratio. Of the three instruments considered, we recommend the MMS1 for use in the application of fruit sorting by NIRS.

Optimising optical configuration and instrument parameters for fruit sugar content calibration

Light angle relative to fruit and detector

The intensity of light detected was not dependent on the angle of incidence of the light beam on the fruit surface (data not shown). This result is explained in terms of the diffuse transmission of light through the fruit, with incident radiation scattered within the fruit such that the angle of incident illumination has little effect.

As expected, the intensity of light detected at a given wavelength (800 nm) decreased as the light beam was moved away from the detected area. The decrease in detector response, R (counts), was described with reference to the distance between the centre of the illuminated area and the detected area of the fruit, D (mm). This exercise was undertaken for an optical arrangement involving a single 50-W halogen lamp and the detector aligned to the centre of the fruit and positioned at 10 cm from the fruit surface (equation 1). The exercise was repeated incorporating a 45-mm-diameter cylindrical shroud between the detector and the fruit surface, to eliminate specular radiation (equation 2).

$$R = 18525\ e^{-0.0668\ D} \quad (R^2 = 0.943) \quad \text{(light without shroud)} \tag{1}$$

$$R = 64646\ e^{-0.085\ D} \quad (R^2 = 0.994) \quad \text{(light shrouded)} \tag{2}$$

Table 1. Calibration (R_c^2 and SEC) and validation (SECV) regression parameters (modified partial least squares procedure) of spectra collected with two spectrometers (MMS1 and S2000) using the same optical and sample presentation system (fibre optic interactance probe)

Calibrations were performed using the second derivative (gap size of 4) of unsmoothed data from the wavelength range 700–1050 nm. Scatter correction was not employed. Four spectra were acquired of each of 16 filter paper bundles, each saturated at different concentration of sucrose, at approximately 1.5-°Brix intervals between 0 and 20

Instrument	Terms (°Brix)	R^2	SEC	SECV
MMS1	2	0.904	1.73	1.85
S2000	2	0.619	3.44	5.40

Thus, moving the detector from 40 to 50° with respect to the light source decreased the observed count from *ca* 24–4% and 7–2% of maximum signal (i.e. detector saturation; 200 ms integration time) for the non-shrouded and shrouded arrangements, respectively.

We had expected that, at lesser angles of light source to detector, higher levels of radiation would be monitored, but that the 'path' of this light would be primarily through exocarp and outer mesocarp tissues. Therefore, increasing incident light to detector angle should allow for proportionally more spectral information on the tissue of interest, the edible mesocarp. However, at some incident light to detector angle, the disadvantage of decreased light transmission (i.e. decreased signal to noise ratio) must outweigh this advantage. Also, as the angle between incident light and detector is increased (particularly beyond 90°); it is expected that proportionally more of the detected light will have penetrated the seed cavity and carry spectral information about seeds, as well as about mesocarp tissue.

Spectra were acquired at four lamp–detector angles for 40 fruit, using a shroud between lamp and fruit (Table 2). Calibration statistics (SEC and related R_c^2, and SECV, after outlier removal) were optimal at a detector–lamp–fruit angle of 60°. For ease of fabrication, an angle of 45° between incident light and detector was adopted in further characterisation of the optical system.

Number of lamps

Increasing the number of lamps was expected to increase the available signal to the detector, and decrease the signal to noise ratio. Aoki *et al.* (1996) reported an optical arrangement employing 16 lamp positions around the equator of the melon fruit, with the detector viewing an area of the fruit at 90° to this plane. However, the use of more lamps will also increase the volume of the fruit 'sampled' by the light, which may degrade a calibration based on the analysis of a relatively small tissue sample in the primary analytical method.

Increasing the number of lamps from one to four had little effect on calibration performance (Table 2). Four lamps were employed in further characterisation of the optical system. These lamps were positioned at 45° in the vertical plane, with respect to the detector, and at 90° intervals in the horizontal plane, with respect to other lamps.

Number of scans per spectra

The SNR of spectra will improve proportionally to the square root of the number of scans averaged per spectrum. Calibration SECV decreased with increased number of scans, although this improvement was marginal and the R_c^2 and related SEC terms were degraded between 4 and 16 scans. Increased scan time will lead to sample change through heating, which could alter spectral characteristics and thus calibration performance (Guthrie and Walsh 1999). However, when fruit were held under the lamps for a period

of 3 min, (fruit internal flesh increased in temperature by less than 1°C, while skin temperature rose by greater than 15°C), calibration performance was not significantly impacted (Table 2). Averaging of four scans per spectra was adopted in further characterisation of the optical system.

Detector 'shrouding' and distance of detector to fruit

Calibration performance was degraded by removal of the shroud between the detector and the fruit surface, in terms of R_c^2, SEC and SECV (Table 2). This result is consistent with the interpretation that the detection of specular and emergent light that has interacted only with the very surface layers (top few millimetres) of the fruit surface degrades calibration performance. The placement of a 40-mm high, 45-mm diameter collar on the fruit under the detector supported a calibration that was apparently superior to the arrangement employing a shroud between detector and fruit surface (Table 2). As both arrangements prevent specular reflections from the fruit surface from reaching the detector, equivalent calibrations were expected. Calibration performance was apparently slightly improved in terms of both calibration R_c^2 and SECV when the distance between fruit surface and detector/light

Table 2. The effect of lamp-fruit-detector angle, a signal filtering routine, number of lights, number of scans averaged per spectrum acquired, and the presence of a shroud between lamp and fruit surface on the calibration of Zeiss MMS1 spectral data (700–1050 nm) to melon flesh Brix, in comparison with two reflectance mode bench top NIR spectrometers
Calibrations were developed for spectra ($n = 40$) acquired of a population of fruit (mean 9.5, standard deviation 1.7°B) for various lamp–detector angles and for three spectrometers, and for spectra acquired of a population of 208 fruit (mean 8.3, standard deviation 1.2°B) for conditions varying with respect to the number of lights, presence of a shroud, and number of scans averaged. The default configuration consisted of shroud between detector and fruit, four lamps mounted to illuminate the fruit at 40° with respect to the detector, and averaging of four scans per spectrum, with a 200-ms integration time per spectrum. Data of treatments marked with an asterisk has been repeated for ease of data comparison. For condition 16b, fruit were held under the lamps for 3 min before scanning. A data treatment of scatter correction (SNV and detrend), second derivative gap size of 4, with no data smoothing was adopted for all calibrations. The Savitzky–Golay filtering routine (SG) was applied to spectra acquired in the assessment of 40° lamp angle. MPLS regressions were performed with all data, and with removal of outlier data as identified using the WINISI chemometric package critical 'H' of 3. The MMS1 was used with a shroud, four lamps illuminating the fruit at 45°, and four scan averaging in the spectrometer comparison exercise. Spectral data over the wavelength range 700–1050 nm, 700–1700, and 700–2300 nm was used from the MMS1, Perten DA 7000 and NIR Systems 6500 spectrometers, respectively

	All data					Outliers removed				
Attributes	*n*	Terms	R_c^2	SEC	SECV	Terms	Outliers	R_c^2	SEC	SECV
Lamp angle (°)										
20	40	1	0.14	0.99	1.15	1	2	0.19	0.97	1.11
40**	40	3	0.64	0.65	1.18	3	0	0.64	0.65	1.18
40SG	40	3	0.05	1.16	1.40					
60	40	4	0.76	0.52	1.96	4	2	0.82	0.43	0.84
80	40	1	0.15	0.99	1.26	4	1	0.38	0.84	1.03
Number of lights										
1	210	7	0.64	0.71	0.90	7	3	0.68	0.68	0.86
2	210	2	0.43	0.92	0.95	6	11	0.61	0.74	0.85
4*	208	6	0.63	0.73	0.88	6	5	0.66	0.69	0.83
Number of scans										
1	210	2	0.45	0.89	0.92	2	3	0.44	0.89	0.92
2	210	2	0.43	0.92	0.95	2	6	0.46	0.88	0.91
4*	208	6	0.63	0.73	0.88	6	5	0.66	0.69	0.83
16a	212	5	0.57	0.78	0.87	6	5	0.63	0.72	0.82
16b	210	6	0.60	0.76	0.84	6	6	0.61	0.74	0.81
Shroud/pathlength										
Shroud on*	208	6	0.63	0.73	0.88	6	5	0.66	0.69	0.83
Collar on	210	6	0.70	0.66	0.81	7	7	0.75	0.58	0.67
Shroud off — fixed path	213	2	0.45	0.89	0.91	2	9	0.47	0.87	0.89
Shroud off — variable path	196	4	0.50	0.84	0.93	3	15	0.51	0.82	0.87
Spectrometer comparison										
MMS1**	40	3	0.64	0.65	1.18	3	0	0.64	0.65	1.18
6500 (–2300)	40	1	0.21	0.95	1.07	2	4	0.51	0.79	1.06
6500 (–1100)	40	4	0.59	0.69	0.97	3	3	0.71	0.55	0.84
Perten (–1700)	40	3	0.60	0.68	1.01	3	2	0.62	0.66	0.62
Perten (–1050)	40	1	0.16	0.99	1.10	1	1	0.97	0.97	1.07

source was allowed to vary in response to fruit size (i.e. by *ca* 50 mm). Such change in fruit diameter altered the effective distance between illuminated and detected regions of the fruit surface. Further, as the detector fibre optic has a numerical aperture of 0.22, an increasing area of the fruit surface is imaged as distance between the probe and the fruit surface is increased. This would result in an increased detector count, offset by a decrease in light intensity. Also, if the field of view of the detector overlaps the areas of direct lamp illumination of the fruit surface, specular reflection will also reach the detector. It was expected that calibration performance should therefore decrease when distance from detector to fruit varied.

Calibration maths

The optimal math treatment of spectral data is expected to be specific to the instrumentation and the application. For example, scatter correction routines (standard normal variance and detrend in the ISI software) are typically applied to reflectance spectra of samples with a rough, light scattering surface. First and second derivative procedures are useful to remove changes in spectral baseline level and slope, and to highlight spectral features. The optimal value for the 'gap' (number of data points) over which the derivative is calculated will depend on the band width of the spectral feature of interest, and the noise and wavelength resolution of the instrumentation used. Data smoothing routines can also be useful in the reduction of noise and elimination of redundant spectral information. An empirical 'test it and see' approach is generally used to establish the best math treatment for a given application. For example, Guthrie and Walsh (1997) established that a math treatment involving second derivative over four data points and smoothing over four data points was optimal in the calibration of sugar content in intact pineapple fruit using NIRSystems 6500 reflectance spectra.

Calibration math treatment was optimised for the populations used in the comparison of optical geometry, with a standard treatment adopted (as used in Table 2). The optimal optical configuration was then used to collect spectra of a large number of fruit (see below). We report here (Table 3) an exercise in comparison of math treatments on this larger population, which yielded similar conclusions but more marked differences than obtained with the smaller population sets.

Table 3. The effect of data treatments (derivative condition and gap size, smoothing, scatter correction) on the calibration of Zeiss MMS1 spectral data (700–1050 nm) to melon flesh Brix

Spectral data is of a population of 1991 fruit (mean 8.1, standard deviation 1.26°B). Values marked with an asterisk represent cases were a smoothing window larger than a derivative gap window

	Data treatment		Scatter correction (SNV and detrend) treatment				Nil scatter			
Derivative	Gap size	Smooth	Terms	R_c^2	SEC	SECV	Terms	R_c^2	SEC	SECV
0	0	1	15	0.55	0.85	0.86	16	0.61	0.78	0.79
0	0	4*	16	0.52	0.87	0.87	16	0.55	0.84	0.86
0	0	10*	15	0.44	0.94	0.95	15	0.48	0.91	0.94
0	0	20*	15	0.31	1.0	1.1	16	0.39	0.98	0.99
1	4	1	15	0.58	0.81	0.84	16	0.64	0.76	0.79
1	4	4*	15	0.50	0.89	0.90	15	0.55	0.85	0.85
1	4	10*	16	0.50	0.89	0.91	15	0.49	0.90	0.91
1	4	20*	15	0.34	1.02	1.04	15	0.40	0.98	0.99
1	10	1	15	0.52	0.87	0.90	15	0.55	0.84	0.87
1	10	4	16	0.50	0.89	0.91	15	0.49	0.90	0.91
1	10	10*	15	0.42	0.96	0.97	15	0.44	0.94	0.96
1	10	20*	14	0.30	1.05	1.07	16	0.39	0.98	1.00
2	4	1	13	0.59	0.81	0.84	15	0.65	0.74	0.77
2	4	4	13	0.54	0.85	0.88	14	0.59	0.80	0.83
2	4	10*	13	0.49	0.90	0.91	14	0.54	0.86	0.88
2	4	20*	12	0.34	1.02	1.03	14	0.41	0.97	0.98
2	8	1	13	0.50	0.89	0.91	14	0.54	0.86	0.87
2	8	4	12	0.44	0.94	0.95	14	0.49	0.90	0.92
2	8	8	15	0.44	0.94	0.96	14	0.45	0.93	0.95
2	8	10*	12	0.39	0.99	0.99	14	0.43	0.95	0.96
2	8	20*	14	0.29	1.06	1.07	14	0.30	1.05	1.06
2	10	1	14	0.50	0.89	0.91	16	0.56	0.83	0.85
2	10	4	14	0.45	0.93	0.95	16	0.48	0.91	0.90
2	10	20*	15	0.29	1.06	1.07	15	0.31	1.04	1.05

Using the ISI chemometric package, outlier spectra were detected and removed from the data set. Approximately 5% of spectra were removed from populations, resulting in a consistent improvement in calibration performance (Table 2). However, as removal of outlier data results in inconsistent population structure, this option was not employed when evaluating math treatments (Table 3). The scatter correction routines (standard normal variance and detrend) decreased calibration performance in terms of SECV and R_c^2 (Table 3). We attribute this result to the optical geometry of the system employed, which was effectively a transmission rather than a reflectance system.

Various signal filtering routines may be used to remove noise from the acquired spectra (e.g. Fourier transform, box car averaging, Butterworth filter). Osborne *et al.* (1999) reported the use of a Butterworth filter improved the development of calibrations of kiwifruit Brix, based on spectra acquired using a Zeiss MMS1 spectrometer. As the Savitsky-Golay signal filter was available within the Zeiss MMS1 test software, we filtered spectra acquired at a lamp–detector angle of 40°. The calibration developed with this data was severely degraded in terms of regression coefficient and SEC (Table 2), and this treatment option was not considered further.

Calibration performance was marginally enhanced by the use of derivatised data (second derivative superior to first or no derivative). The best calibrations achieved using 'raw', first and second derivative data yielded a SECV of 0.79 (no smoothing), 0.79 (derivative gap of 4 data points, no smoothing) and 0.77 (derivative gap of 4 data points, no smoothing), respectively. We attribute the relative lack of calibration response to the use of derivatives to the transmission optical geometry of the system employed. Derivatives should offer more value in reflectance systems in which baseline shifts between samples can be large.

Calibration performance was degraded as the gap over which the derivative was calculated was increased from 4 to 8 to 10 (Table 3). Calibration performance was also degraded by smoothing of data. The Zeiss MMS1 has a pixel resolution of 3.3 nm, and thus smoothing or derivative calculated over four data points involves averaging of data over a 13-nm spectral range, equivalent to the wavelength resolution of the instrument. Further averaging will involve loss of spectral information. Also, the MMS1 has a high SNR, such that the effect of signal averaging (smoothing) to signal precision may not contribute to improved calibration performance. Smoothing over a greater gap than used in the calculation of the derivative is expected to result in a loss of information, and a slight degradation in calibration performance was observed.

Based on the above observations, we recommend a data treatment of second derivative over a gap size of four, with no scatter correction or smoothing, for this instrumentation and optical configuration.

Design of field unit for consideration of calibration robustness

In summary, the following instrument design is proposed for the non-invasive assessment of melon using a low-cost, commercially available spectrometer module: the Zeiss MM1 spectrometer used with a shroud (45 mm diameter, 100 mm length) between the detector fibre optic and the fruit surface, and four 50-W tungsten halogen lamps and lamps mounted at 90° intervals, positioned 100 mm above the fruit and aligned with the approximate centre of the fruit (i.e. angle of 45° between light incidence and detected area of fruit). These features have been adopted in a 'luggable' or 'at-line' NIR system that can be transported between pack-houses. This unit incorporates a spring-loaded platform to keep the fruit firmly against the detector shroud, while allowing for ease of fruit change-over. The outside dimensions of the unit are 400 (width) by 400 (depth) by 550 mm (height), accommodating one melon at a time, and locating the spectrometer and other electronics above the sample chamber.

The following operational parameters are recommended for the use of this hardware: an integration time of 200 ms, as required to achieve a detector response at *ca* 50% of saturation, with detector and lamp powered up 2 h before use to ensure instrument stability. Averaging of four scans per spectra is recommended to improve signal to noise ratio. A 'default' data treatment of second derivative calculated over four data points, without further data pre-treatment, is suggested. We have subsequently developed a LabView (National Instruments, West Hartford, CT, USA)-based spectral acquisition and analysis package that allows application of calibrations to give predictions in a real-time basis.

The system described was benchmarked in terms of calibration performance against two commercial research-grade NIR spectrometers, operated over the full NIR wavelength capability of these instruments and in reflectance mode (Table 2). The purpose-built instrumentation supported a calibration inferior to that achieved using the Perten DA7000 and NIRSystems 6500 operated over a similar wavelength range. However, the purpose-built instrumentation is recommended as a field-suitable, low-cost alternative. The relatively good performance of the purpose-built instrumentation is ascribed to the low SNR of the MMS1 detector and optimisation of the system in terms of optical geometry of incident light, sample and detector. We will employ this system to collect spectra of melons of various cultivars, growing districts and seasons to further develop the consideration of Guthrie *et al.* (1998) of calibration robustness. Harvested rockmelon fruit vary between 6 and 14°Brix, with 10°Brix commonly accepted as a quality standard. Low-cost instrumentation that supported a standard error of prediction of less than 1oBrix on intact melons would find ready acceptance in the Australian melon industry for pack-house grading of fruit. Further, equipped with a robust calibration,

this instrumentation should be useful in physiological, agronomic and breeding programs targeting melon fruit soluble solids content.

Acknowledgments

The instrumentation work was supported by an Australian Research Council grant while the calibration work was supported by a Horticultural Research and Development Corporation Grant. We thank Elan Horticultural for use of the Oriel–Larry instrument.

References

Aoki H, Kouno Y, Matumoto K, Mizuno T, Maeda H (1996) Non-destructive determination of sugar content in melons and watermelon using near infrared (NIR) transmittance. In 'Proceedings of the international conference on tropical fruit, Kuala Lumpur 23–26 July, 1996'. (Eds S Vijaysegaran, M Pauziah, MS Mohamed and S Ahmad) pp. 207-218. (Malaysian Agricultural Research and Development Institute: Kuala Lumpur, Malaysia)

Bellon V, Vigneau JL, Leclerccq M (1993) Feasibility and performances of a new, multiplexed, fast and low-cost fibre-optic NIR spectrometer for the on-line measurement of sugar in fruits. *Applied Spectroscopy* **47**, 1079–1083.

Bellon-Maurel V, Vigneau JL (1995) NIR fast spectrometer for fruit internal quality assessment: reproducibility study. In 'Proceedings of harvest and postharvest technologies for fresh fruit and vegetables. Guanajuato, Mexico, Feb. 1995'. (Eds L Kushwaha and R Serwatowski) pp. 471–476. (American Society of Agricultural Engineers: St Joseph, MI, USA)

Dull GG, Birth GS, Smittle DA, Leffler RG (1989) Near infra-red analysis of soluble solids in intact cantaloupe. *Journal of Food Science* **54**, 393–395.

Dull GG, Leffler RG, Birth GS, Smittle DA (1992) Instrument for non-destructive measurement of soluble solids in honeydew melons. *Transactions of the ASAE* **35**, 735–737.

Greensill CV, Walsh KB (2000) Optimisation of instrument precision and wavelength resolution for the performance of NIR calibrations of sucrose in a water-cellulose matrix. *Applied Spectroscopy* **54**, 426–430.

Guthrie J, Walsh K (1997) Non-invasive assessment of pineapple and mango fruit quality using near infra-red spectroscopy. *Australian Journal of Experimental Agriculture* **37**, 253–263.

Guthrie J, Walsh K (1999) Influence of environmental and instrumental variables on the non-invasive prediction of Brix in pineapple using near infrared spectroscopy. *Australian Journal of Experimental Agriculture* **39**, 73–80.

Guthrie J, Wedding B, Walsh K (1998) Robustness of NIR calibrations for soluble solids in intact melon and pineapple. *Journal of Near Infrared Spectroscopy* **6**, 259–265.

Kawano S (1994) present condition of non-destructive quality evaluation of fruits and vegetables in Japan. *Japan Agricultural Research Quarterly* **28**, 212–216.

Jaenisch HM, Niedzwiecki AJ, Cernosek JD, Johnson RB, Seeley JS, Dull GG, Leffler G (1990) Instrumentation to measure the near-IR spectrum of small fruits. *Optics in Agriculture. Proceedings of the International Society of Optical Engineering* **1379**, 162–167.

Mowat AD, Poole PR (1997) Use of visible near infrared diffuse reflectance spectroscopy to discriminate between kiwifruit with properties altered by preharvest treatments. *Journal of Near Infrared Spectroscopy* **5**, 113–122.

Oriel (1997) 'Oriel Corporation light sources, monochromators and spectrographs, detectors and detection systems, fiber optics (catalogue).' (Oriel Corporation: Stratford, CT, USA)

Osborne SD, Künnemeyer R, Jordan RB (1999) A low-cost system for the grading of kiwifruit. *Journal of Near Infrared Spectroscopy* **7**, 9–15.

Peiris KHS, Dull GG, Leffler RG, Kays SJ (1998) Near infra-red spectrometric method for nondestructive determination of soluble solids content of peach. *Journal of the American Horticultural Society* **123**, 898–905.

Manuscript received 26 July 1999, accepted 14 August 2000